Mid-summer fish behavior in a high-latitude twilight zone

Stein Kaartvedt ©,* Svenja Christiansen ©, Josefin Titelman ©
Department of Biosciences, University of Oslo, Oslo, Norway

Abstract

The behavior of the mesopelagic fish *Benthosema glaciale* was studied at 60°N in mid-summer. We hypothesized that diel vertical migration (DVM) is constrained by short and dusk nights (surface illumination $> 10^{-2} \, \mu$mol m^{-2} s^{-1}) and that individuals are active at depth during the long summer days. Submerged echosounders provided high-resolution data throughout the water column. During the day, a part of the population ascended toward the increasing daylight. Short vertical relocations were followed by minutes of vertical inactivity. Swimming included horizontal turns and loops associated with the vertical steps. Normal DVM was initiated ~ 4 h before sunset and reflected independent individual decisions. The fish initially ascended stepwise but switched to mostly straight upwards swimming attaining 3–4 cm s^{-1}. Their vertical speed was faster than the slow ascent of isolumes and even the deepest living fish potentially could reach upper layers shortly after sunset. However, many individuals aborted their ascent and returned to depth before the darkest time of the night, while others returned downward closer to sunrise. The daytime swimming and individual variability in diel migration behavior have implications for encounters with prey and predators in the twilight zone and the biological carbon pump. A principal conclusion is that mesopelagic fishes can modify their behavior and migration patterns to suit a wide range of changing conditions.

Mesopelagic fishes worldwide carry out diel vertical migrations (DVM), often studied as vertical movements of acoustic scattering layers (Bianchi and Mislan 2016; Klevjer et al. 2016). The widely accepted explanation for this behavior is that the fishes ascend to feed at night and descend to hide in the faintly illuminated twilight zone during the day (Hays 2003). However, the proportions of the populations taking part in the vertical migrations vs. those remaining at depth vary (Klevjer et al. 2016). Taxonomy, environmental characteristics, and individual state and motivation all influence behavior, including vertical migrations (Pearre 2003; Bos et al. 2021; Pinti et al. 2022). Extremes in migratory behavior are represented by scattering layers ascribed to *Cyclothone* spp. which do not migrate vertically (Olivar et al. 2012; Peña et al. 2020;

Sarmiento-Lezcano et al. 2022), and scattering layers in the Red Sea, where entire populations of mesopelagic fishes always carry out DVM (Sobradillo et al. 2022).

To what degree individual antipredation responses like DVMs are plastic appears key to the organisms' ability to adjust their behavior in response to global change (Pinti et al. 2022). Moreover, establishing the role of behavior, with a particular focus on deep-sea processes, is of paramount importance in understanding the biological carbon pump (Pinti et al. 2022). Mesopelagic fishes may be torpid during the day (Barham 1971; Belcher et al. 2020), drifting passively with the currents (Kaartvedt et al. 2009). However, Barham (1971) also referred to active mesopelagic fishes at depth, and Sobradillo et al. (2022) documented that mesopelagic fishes in the Red Sea were continuously moving during the daytime. Motility has implications not only for the individual but also for the ecosystem functioning at large (Kays et al. 2015). Activities at mesopelagic depth affect respiration (Torres et al. 1979), predator–prey interactions (Gerritsen and Strickler 1977; O'Brien et al. 1990), and ultimately the biological carbon pump (Davison et al. 2013; Belcher et al. 2019; Saba et al. 2021). Consequently, understanding the ecology of mesopelagic fishes and the related ecosystem impacts requires knowledge of their behavior throughout the diel cycle.

The lanternfish *Benthosema glaciale* is a prevalent component of the mesopelagic acoustic scattering layer in the northern Atlantic (Godø et al. 2009; Pepin 2013; Norheim et al. 2016),

---

*Correspondence: stein.kaartvedt@ibv.uio.no

Additional Supporting Information may be found in the online version of this article.

Author Contribution Statement: S.K. conceived the study, was responsible for the data acquisition and wrote the first draft. S.C. conceived the ideas for and performed the data analyzes as well as being responsible for the visual presentations. S.C. also contributed significantly in the writing. J.T. contributed significantly in the writing, including with conceptual inputs. All authors have approved the final submitted manuscript.

yet with a wider geographic distribution including waters off Western Africa and the Mediterranean (Olivar et al. 2012, 2017). Both its tendency to migrate and its DVM pattern vary throughout the year, and include normal DVM as well as inverse DVM within the twilight zone (Dypvik et al. 2012*a*). During the summer, normal DVM appears common (Sameoto 1988; Pepin 2013; Hudson et al. 2014). However, summer nights are short and light at high latitudes. Therefore, behavioral solutions suitable for mesopelagic fishes at low and mid-latitudes do not necessarily apply to deep-water systems at higher latitudes. Sameoto (1989) suggested that short summer nights in Davis Straight, Canada (∼ 62°N), might limit nocturnal feeding migrations of *B. glaciale* and hence viable populations further to the north. Correspondingly, mesopelagic scattering layers holding *B. glaciale* became progressively weaker and upward migration amplitudes smaller along a northward transect in the Norwegian Sea, extending to ∼ 67°N in May (Norheim et al. 2016). Kaartvedt et al. (2008) hypothesized that mesopelagic fishes at even higher latitudes become constrained by the photoperiod, with feeding impeded by the extreme light climate. Mirroring the light summer nights, the dark winter days may hamper daytime foraging (Kaartvedt 2008). Mechanistic models using *B. glaciale* to assess climate effects on vertically migrating mesopelagic fishes at high latitudes concluded that their poleward distribution is constrained since foraging fishes would be exposed to visual predators in sunlit upper waters at night also (Ljungström et al. 2021; Langbehn et al. 2022). On the other hand, Proud et al. (2017) suggest that mesopelagic fishes will move poleward as the oceans warm, and Chawarski et al. (2022) provided evidence that low temperatures define the biogeographic boundaries of mesopelagic fishes at high latitudes.

B. glaciale and *Maurolicus muelleri* are the dominant mesopelagic fishes in Norwegian fjords. The more shallow-living *M. muelleri* has eyes adapted for dusk foraging (de Busserolles et al. 2017). At 60°N, *M. muelleri* omits its normal "midnight" sinking in early summer as nocturnal irradiance becomes sufficient for visual search (Prihartato et al. 2015). As nights become even lighter ($\sim 10^{-2}$ to 10^{-1} μmol m^{-2} s^{-1}) and shorter in mid-summer, or further north, *M. muelleri* switches to nocturnal schooling in upper waters (Kaartvedt et al. 1998; Prihartato et al. 2015). *B. glaciale* lives deeper, is more dark-adapted, and appears associated with light levels of $< 10^{-6}$ μmol m^{-2} s^{-1} during daytime (Røstad et al. 2016). Therefore, while dusk summer nights may extend the foraging period for *M. muelleri*, we hypothesize that summer nights, in contrast, constrain the nocturnal foraging period of *B. glaciale*. Nights are short and may be too light to allow the fishes to enter the uppermost layers, where their prey abound in summer. We, therefore, hypothesize that daytime activity in the twilight zone becomes key in the life of *B. glaciale* and other dark-adapted mesopelagic fishes when summer days are long and DVM is constrained.

We here address the behavior of acoustic targets ascribed to *B. glaciale* during day and night in mid-summer at 60°N. We analyze data from echosounders submerged at three depths to obtain simultaneous high-resolution data throughout the water column. Our approach enables close-up observation of individual behavior in the remote, mesopelagic habitat, in contrast to most acoustic studies that detect mesopelagic scattering layers from a distance. We assess DVM behavior in different parts of the water column and provide quantitative descriptions of individual swimming behavior in the twilight zone. The establishment of the level of variability of behaviors without the confounding influences from multispecies assemblages is generally difficult to achieve for mesopelagic fauna. Therefore, while addressing one particular species in a single location, the findings provide novel and general information on the activity and intraspecific variation in behavior within a population of mesopelagic fish.

Methods

Study location and data collection

We studied mesopelagic fishes in Masfjorden, Norway (60°5′N, 5°3′E). The maximum depth is 490 m and an outer sill at 75 m hampers the exchange of the deep basin water with adjacent regions. Temperature and salinity are homogenous beneath the sill depth, with values of 7–8°C and ∼ 35, respectively. The basin water was well oxygenated during the study period at ∼ 4 mL O$_2$ L^{-1} (Aksnes et al. 2019).

We made continuous acoustic records from October 2010 to August 2011 (Kaartvedt et al. 2021). We here analyze data from 10 to 30 June 2011 during a period where minimum nocturnal surface irradiance was 10^{-2} to 10^{-1} μmol quanta m^{-2} s^{-1} (Prihartato et al. 2015) and the period between sunset and sunrise was ∼ 5 h. We deployed three upward-looking SIMRAD EK60 split-beam echosounders (7.1° beam angle), mounted at the bottom (38 kHz; ∼ 375 m; pulse length 512 ms; 1 ping s^{-1}) and in rigs floating at ∼ 280 m (120 kHz; pulse length 256 ms; 1–2 pings s^{-1}) and ∼ 90 m (200 kHz; pulse length 128 ms; 1–2 pings s^{-1}). Cables to the shore provided unlimited power and data storage capacity. The echosounders were calibrated at the surface before deployment, using standard methods (Foote et al. 1987).

Identities of acoustic targets

The mesopelagic scattering layers in Masfjorden persist over time and have been repeatedly identified (Giske et al. 1990; Staby et al. 2011; Underwood et al. 2021). During the daytime, *M. muelleri* forms acoustic scattering layers in the upper 150 to 200–250 m. There is a likely inclusion of smaller *B. glaciale* toward the lower part of this range, but their relative contribution is uncertain (Rasmussen and Giske 1994; Staby et al. 2011; Christiansen et al. 2021). Size increases with depth (Dypvik et al. 2012*b*), as also found for *B. glaciale* elsewhere (Halliday 1970; Roe and Badcock 1984). The largest fish occur

below 300 m, where the dominant mode of *B. glaciale* captured by Dypvik et al. (2012*b*; September/October) ranged from 5.5 to 7.8 cm (daytime sampling depth at 300–400 m). They found an additional mode at 3.5–5.4 cm at depths corresponding to our records by the 120 kHz echosounder (daytime sampling depth at 200–300 m). Trawl samples from the start and end of our 10-month registration period (Christiansen et al. 2021) concurred with previous studies, indicating that *B. glaciale* is the main cause of backscattering deeper than 250 m. Correspondingly, mesopelagic fish displaying a saltatory "glide and pause" behavior were by far the most common organisms in video records from the deep scattering layer (> 275 m) of Masfjorden (Underwood et al. 2021). The individuals identified to species were all *B. glaciale*. These camera observations in winter unveiled few siphonophores in this layer (potential acoustic targets; Barham 1966, Proud et al. 2019), and confirm that the deep scattering layer in this fjord—persistent over seasons and years—is present in spite of low abundance of siphonophores. However, the potential presence of physonect siphonophores cannot be ruled out. They are consistently under-sampled by trawls (Hetherington et al. 2022), are present in nearby fjords in summer (Hosia and Båmstedt 2008) and some siphonophores has context-specific swimming modes that resemble those of fishes (Du Clos et al. 2022).

Pelagic shrimps, particularly *Sergestes arcticus*, are numerous in deep trawl catches but are weaker acoustic targets than the fish. The scattering layers at 38 kHz and 120 kHz here ascribed to *B. glaciale* are consistent over time and also appear at 18 kHz (Kaartvedt et al. 2008), while invertebrates like shrimps give little backscatter at such a low frequency (Love et al. 2004). Shrimplike targets are moreover directional, that is, target strength (TS) varies considerably with vertical orientation (Greenlaw 1977). The, apparently, neutrally buoyant targets addressed here (*see* "Results" section) displayed little variation in acoustic backscatter with vertical swimming direction, which is characteristic of targets where a small swim bladder provides the bulk of the echo (Fujino et al. 2009). TS values measured in the current study appear reasonable compared with previous assessments for *B. glaciale* at 38 and 120 kHz (Scoulding et al. 2015). Summing up the evidence, we are confident in the species identification within the twilight zone.

We here also refer to individuals recorded above 90 m by the 200 kHz echosounder at night. We do not have trawl samples during mid-summer nights. During this time *B. glaciale* and *M. muelleri* may co-occur in upper waters and siphonophores are common in upper layers of Norwegian fjords (Hosia and Båmstedt 2008). The high-frequency shallow-most echosounder will also record targets like vertically migrating shrimps. We used behavioral information for assessing target identity, but ascribing upper water targets to *B. glaciale* is uncertain because of the mix of targets that may co-occur and thus merely represents suggested target identities.

Data selection

All data were used in objective quantitative analyses. In addition, we present example echograms comparing behavior in sunny and foul weather as daytime irradiance varied by nearly one order of magnitude between days (e.g., Figure 1). We also present echograms at varying resolutions to describe vertical swimming patterns. All echograms and figures were made in MATLAB (MathWorks; R2021b).

A stationary split-beam echosounder in a low-advective environment can record numerous recurrent echoes from an individual as it traverses the acoustic beam. This enables assessment of individual vertical behavior by following individual echo traces on the echogram and individual 3D behavior by applying acoustic target tracking (Brede et al. 1990).

To provide qualitative measurements of vertical migration speeds, we visually located echo traces on the echograms (c.f. Fig. 2). We obtained the start and end depths and times of the traces by zooming into the echogram in MATLAB and marking and saving the respective data points. Then, we determined vertical speeds based on the depth change over time. There is no range limitation in using this approach, except for the need for visually detecting the targets on the echogram.

In contrast, requirements for data quality in target tracking limit the range of study (distance to the echosounder). This is because the larger volume by range increases the probability of overlapping (multiple) targets, particularly at high numerical density. Target tracking also may include range-dependent biases in the assessment of TS and horizontal swimming. Signal-to-noise ratios become weaker, the instrument resolution becomes coarser and the wider acoustic beam by range facilitates a longer retention time of organisms within the acoustic beam (Christiansen et al. 2022). The selection of range, therefore, embodies the trade-off between obtaining sufficiently high numbers of targets and the quality of representative data.

Target tracking and post-processing of tracking data

We used Sonar5-Pro (Balk 2019) to perform the target tracking as in Christiansen et al. (2019). To improve single echo detections by improving signal-to-noise ratios, we first applied a cross-filter detector (Balk and Lindem 2002). We then applied automatic target tracking with the parameters shown in Supporting Information Table S1 for ranges between 5 and 15 m for 120 kHz and 10–40 m for 38 kHz, obtaining vertical range (m); and horizontal (X and Y [m]; distance from mid-beam positions) and TS (dB re 1 m^2) for each target.

We post-processed the track data as in Christiansen et al. (2022), which included ping gap interpolation, outlier removal, splitting of multiple targets, current subtraction, and smoothing by a lowess (locally weighted linear regression) smoother. We interpolated over ping gaps (maximum ping gaps were restricted to three pings) by applying Piecewise Cubic Hermite Interpolating Polynomial interpolation (*pchip*; MATLAB function *interp1*) over time using the median
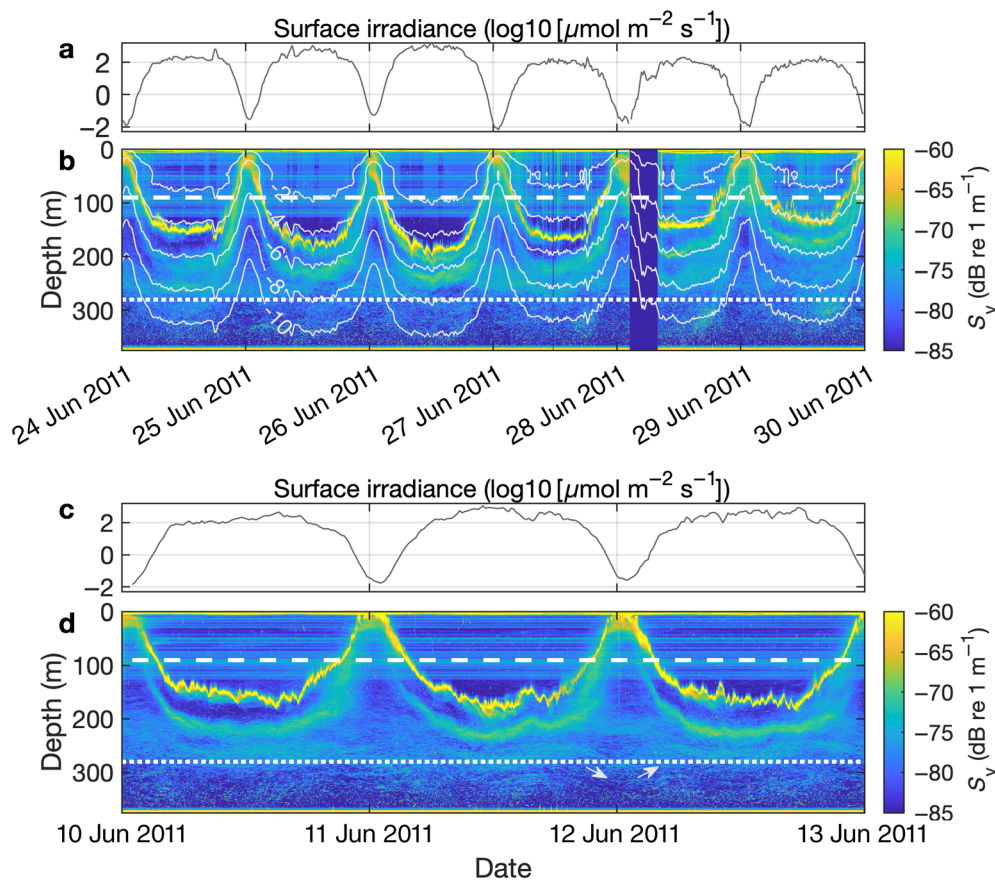
Fig. 1. Surface irradiance (**a**) and (**c**) and vertical distribution of backscatter (S_v; dB re 1 m^{-1}) from bottom-mounted 38 kHz echosounder (**b**; missing data early night 28 June) and (**d**) in Masfjorden, June 2011. Light gray lines in (**b**) depict isolumes. White horizontal dashed lines indicate the location of the 200 kHz echosounder, and the white dotted lines the location of the 120 kHz echosounder. Arrows in (**d**) indicate the vertical displacement of the backscatter.

ping interval (~ 1 s). We defined outliers as values (X, Y, and range) that exceeded the running median absolute deviation (window size 10 data points) within the track more than 10-fold and replaced those values with the running median (window size 10 data points). We identified and split potential multiple targets in several steps. First, we fitted a *lowess* smoother to each track's X and Y values (window size 18 and 30 for 120 and 38 kHz, respectively). Then, for each track, the X and Y residuals were calculated and the residual spread was determined, defined as the 98th percentile of the residuals obtained by interpolation. We then calculated the median residual spread of all tracks. Finally, we split all tracks at positions where X or Y values exceeded the fit $\pm$ the median residual spread and retained all track fragments > 20 data points.

Currents and other water movements may bias velocities obtained from target tracking. Therefore, we calculated and subtracted the binned (2 m by 36 min, >3 tracks per bin) net horizontal population movement. This procedure is based on the assumption that the mesopelagic fishes generally move independently and that net movements in the same direction

are due to currents, thus potentially masking any "real" coordinated behavior. Estimated median current speeds were ca. 0.9 cm s^{-1}, 95th percentile ca. 2 cm s^{-1}, with maximum ca. 5.3 cm s^{-1}, concurring well with previous estimates (Kaartvedt et al. 2009). Finally, all tracks were smoothed, the horizontal positions by lowess smoothing using smoothing windows of 6 and 10 for 120 and 38 kHz, respectively. The range was smoothed by a running mean with window sizes 6 and 3 (corresponding to ca. 6 s) for 120 and 38 kHz, respectively. The TS was smoothed by a running median with the same window sizes.

Analyses of individual behavior

We here focus mainly on the track data obtained at 120 kHz for a detailed assessment of the 3D swimming patterns and speed over the 24-h cycle. Tracking was less precise at 38 kHz, but some results on 3D swimming are included here for comparing behavior in mid-waters and near-bottom. Visual scrutiny of individual echo traces (records on echograms) and tracks justified the comparison for the targets ascribed to *B. glaciale* at both frequencies. We subset the
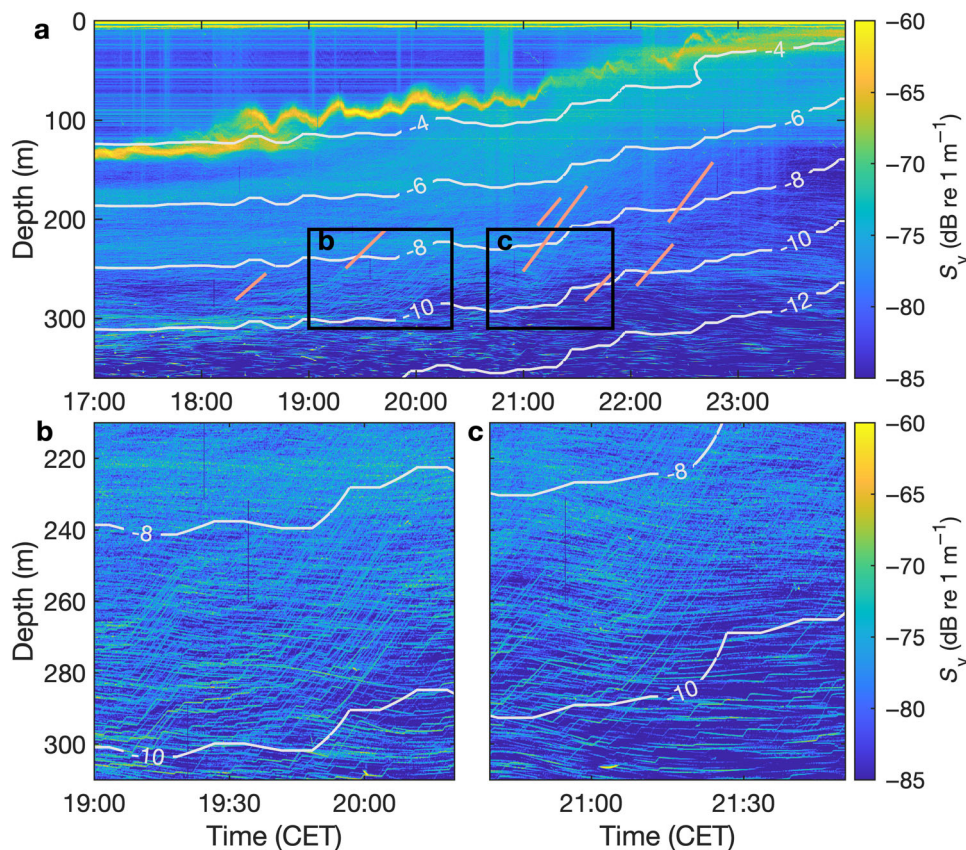
Fig. 2. Individuals ascending in the afternoon on 28 June 2011 (38 kHz). Light gray lines indicate isolumes (log10[μmol m^{-2} s^{-1}]). The red lines highlight individual echo traces.

dataset to tracks with median TS between −70 and −60 dB at 120 kHz and TS between −65 and −50 dB at 38 kHz based on the prevalence of these TS values in individuals identified as *B. glaciale* from echo traces (Supporting Information Fig. S1) and in previous studies (Dypvik et al. 2012*a*).

We tracked the vertical and horizontal swimming patterns. The fish moved in a vertical stepwise (stop-and-go) pattern, and we assessed swimming speed during vertical relocations (steps; defined as vertical swimming speeds > 1 cm s^{-1} over at least three consecutive pings based on scrutiny of large numbers of tracks), step duration, as well as average swimming speed that also accounts for pauses. We established a "vertical activity index" as the time a target spent swimming in steps relative to the time spent in pauses (i.e., summed step durations divided by summed pause durations). When target densities are high, the acoustic target tracking may lead to shorter tracks and pause durations due to splits at overlapping tracks. Therefore, pause and step durations may partly be underestimated here. However, excluding tracks from regions with higher density did not significantly influence the results.

We determined the TS for individuals leaving in the afternoon to assess any size differences between fish initiating

DVMs early and late in the evening. Here, we used tracks from fish ascending at a median vertical velocity > 1 cm s^{-1} and with a minimum duration of 20 s, including all data for the entire period. The required speed and duration were determined empirically by comparing tracks and echo traces on the respective echograms. Tracks were selected from the TS interval defined as originating from *B. glaciale*, that is, −70 to −60 dB at 120 kHz (Supporting Information Fig. S1). We first calculated the median TS for each track and then fit a simple linear regression of those values over time of day (MATLAB *fitlm*). Tracking was less feasible by the bottom mounted 38 kHz echosounder, but data one afternoon (28 June) enabled addressing fast ascending targets over 4 h. We then applied target tracking between 255 and 305 m (range from transducer 70 to 140 m) on targets ascending by more than 1 m at > 1 cm s^{-1}.

To assess horizontal swimming, we calculated both the horizontal speed and the tortuosity, an estimate for turning. The instantaneous horizontal speed was obtained by dividing the Euclidean distances between consecutive horizontal positions by the respective time interval. We established the tortuosity of tracks, following Sobradillo et al. (2022). The tortuosity is a measure of turning where a value of 1 indicates a straight

path, and a tortuosity of 2 indicates that the target swims twice the distance needed to move between two locations. We also provide examples of the 3D swimming paths and speeds of selected individuals.

We binned the track speeds, tortuosity, and step properties to provide a quantitative overview of the activity over depth and time. All times are reported in central European time (CET; UTC + 1). For net ascending and descending tracks, we calculated the mean vertical and horizontal track speed and tortuosity in 0.5 m and 30-min bins with each half a bin width overlap, averaged over all days between 10 and 30 June 2011. We also calculated the mean step speed, step duration, and pause duration for each track and then binned those values by averaging, as above.

Behavior as related to light

We compared our activity data to light measurements. A calibrated LI-190 quantum sensor continuously recorded photosynthetic active radiation (PAR, 400–700 nm) at the surface, and the data were stored on a LI-1400 data logger (Aksnes 2021). Light measurements also included a vertical profile of underwater irradiance obtained around noon on 16 June by a RAMSES ACC hyper-spectral radiometer (Trios-optical sensors, Oldenburg, Germany; Aksnes 2021). Measurements were made down to 90 m. For depths below, we extrapolated by using attenuation coefficients that were estimated for depths deeper than 50 m. We calculated the attenuation coefficient (Kz) for downwelling irradiance (PAR) and approximations for ambient light as in Prihartato et al. (2015) and Christiansen et al. (2021).

Results

Migration of scattering layers

The same basic migration patterns appeared throughout the study period from 10 to 30 June, though with some variation related to changing weather, exemplified here for 24–30 June (Fig. 1). An upper, narrow scattering layer (*M. muelleri*) continuously relocated throughout the day, with the deepest daytime distribution extending to ~ 140–200 m around noon, depending on fluctuating irradiance (i.e., weather; Fig. 1a,b). The layer coherently migrated to surface waters at night. A weaker deeper layer extending to 180–240 m displayed a similar pattern (Fig. 1b).

More diverse migration behavior appeared in mid-waters at ~ 250–300 m (Fig. 1d). These records, ascribed to *B. glaciale*, indicated both normal DVM as well as organisms ascending in the afternoon and then turning in the evening, again ascending in the morning (Fig. 1).

Records in waters > 300 m (ascribed to *B. glaciale*) suggested a varying degree of ascent in the afternoon. Ascent was most prominent during the darker days in foul weather towards the end of the registration period (Fig. 1b), as better illustrated by

higher resolution, displaying individual echo traces (Fig. 2; Supporting Information Fig. S2).

Individual vertical behavior (echo traces)

Migrations from near-bottom waters as recorded by the 38 kHz echosounder were not synchronous. Individuals started ascending ~ 4 h before sunset (22:15 CET), with most of the migrating individuals having left their daytime habitat 1 h before sunset (Fig. 2; an example from a day when irradiance was low; Fig. 1). We did not find any change in TS from early to late starters for the migration sequence depicted in Fig. 2, as derived from the tracks recorded between 255 and 305 m depth by the bottom-mounted echosounder ($n = 64$, simple linear regression slope $= -3.9$, p-value $= 0.45$, adjusted $R^2 = -0.0069$). The median TS was -54.7 dB, and the mean (calculated in the linear domain) was -54.8 dB ± 1.7 dB standard deviation at 38 kHz.

The ascent began stepwise (Fig. 2), but switched to straighter upwards swimming, sometimes intermitted with pauses. Traces of ascending individuals could be discerned up to ~ 130 m depth, corresponding to > 200 m range from the bottom-mounted echosounder. Migration speeds of directly ascending individuals between ca 200 and 300 m depth were on average ($\pm$ SD) 3.3 (± 0.6) cm s^{-1} ($n = 202$) on the dark day depicted in Fig. 2. A corresponding exercise from a brightly illuminated day (26 June; Fig. 1) gave comparable speeds, 3.7 (± 0.7) cm s^{-1}, but fewer registrations ($n = 38$) and later initiation of ascent (*see* details in Supporting Information Fig. S2).

Surface irradiance between early (18 CET h) and late (22 CET h) initiation of upward swimming decreased by about 1.6 orders of magnitude. The vertical speed of ascending individuals was faster than the ascent of isolumes (Fig. 2). This contrasted the *M. muelleri* layer, which ascended in concert with the reduced light intensities, that is, the strong scattering layer roughly associated with the $\sim 10^{-4}$ μmol m^{-2} s^{-1} isolume (Figs. 1, 2). There was no apparent pulse of organisms descending into near-bottom waters in the morning.

Nocturnal ascent as recorded by the echosounder floating at 280 m (120 kHz) started before sunset and the period for initiation of ascent spanned several hours. Still, there was a clear upward pulse in the evening, as exemplified by echo traces one afternoon (Fig. 3). There was no change in TS in the course of the afternoon in ascending tracks between 10 and 30 June, as recorded by the target tracking between 265 and 275 m ($n = 1236$, simple linear regression slope $= -0.23$, p-value $= 0.69$, adjusted $R^2 = -0.0007$; Supporting Information Fig. S3). Likewise, the return descent extended over several hours. While some fish returned to depth before midnight, that is, before the darkest time of night, there was a downward pulse of migrating fish in the morning (Fig. 3).

There was a mixture of stepwise descending and ascending individuals during daytime (Fig. 4). The proportion of ascending individuals increased throughout the day (*see* below).
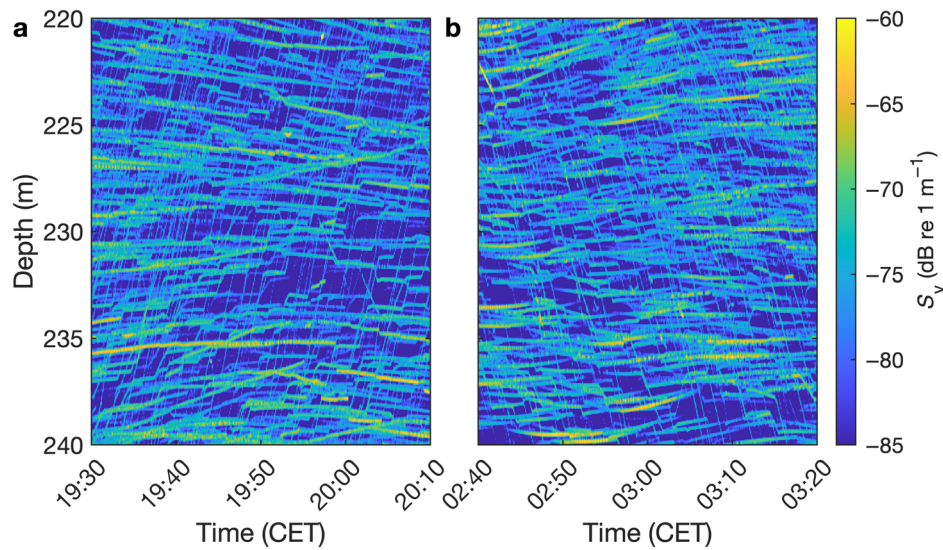
Fig. 3. Echograms (120 kHz) showing prevailing upward (**a**) and downward (**b**) migration on 10 (**a**) and 11 (**b**) June 2011. Sunset at 22:16 h and sunrise at 03:06 h.

The 200 kHz echosounder was located above the mesopelagic zone (at 90 m), and therefore only provided data on mesopelagic organisms at night. Some stepwise vertically migrating individuals from the deeper layers reached shallow waters (Fig. 5; here depicted during descent) and were discernable to depths of 30–40 m.

Quantitative analyses of individual swimming behavior within the twilight zone

Swimming within the track window for the 120 kHz echosounder (265–275 m) was mostly upward from ∼ 07–21 CET (Fig. 6), although descending tracks were also present throughout the day (Fig. 7). Before noon, the ascending individuals were swimming towards increasing light intensity (Figs. 6, 7).

The stepwise vertical swimming in mid-waters included long pauses (Fig. 4), and low average vertical speeds < 0.5 cm s^{-1} (Figs. 6, 7). However, the 95th percentile of average swimming speeds reached 2–3 cm s^{-1} during the main periods of ascent and descent (Fig. 7). The fishes moved throughout the day (Figs. 6, 7). The vertical activity and relocation speeds depended on the durations of steps and pauses as well as on the vertical relocation speed during steps (Fig. 7). The activity index assessed as step duration/pause duration was ∼ 0.2 for all data from 09 to 18 CET (Fig.7) meaning that four of five fishes would be pausing at any time. Pauses were shorter, step duration longer, and vertical swimming faster during the main periods of ascent in the afternoon and descent in the morning (Fig. 7). Pause durations were the longest at night (Fig. 7).
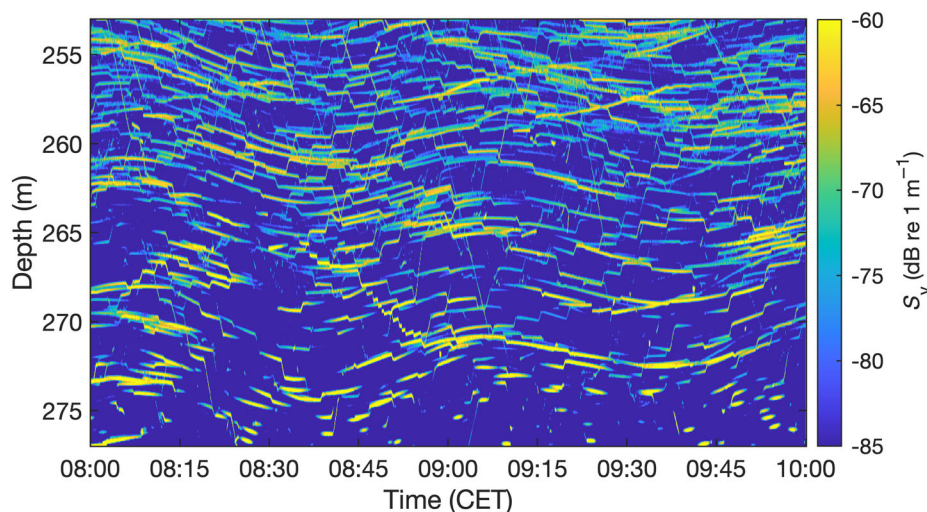

Fig. 4. Echogram (120 kHz) displaying a mixture of descending and ascending individuals during daytime as well as internal waves (25 June 2011).
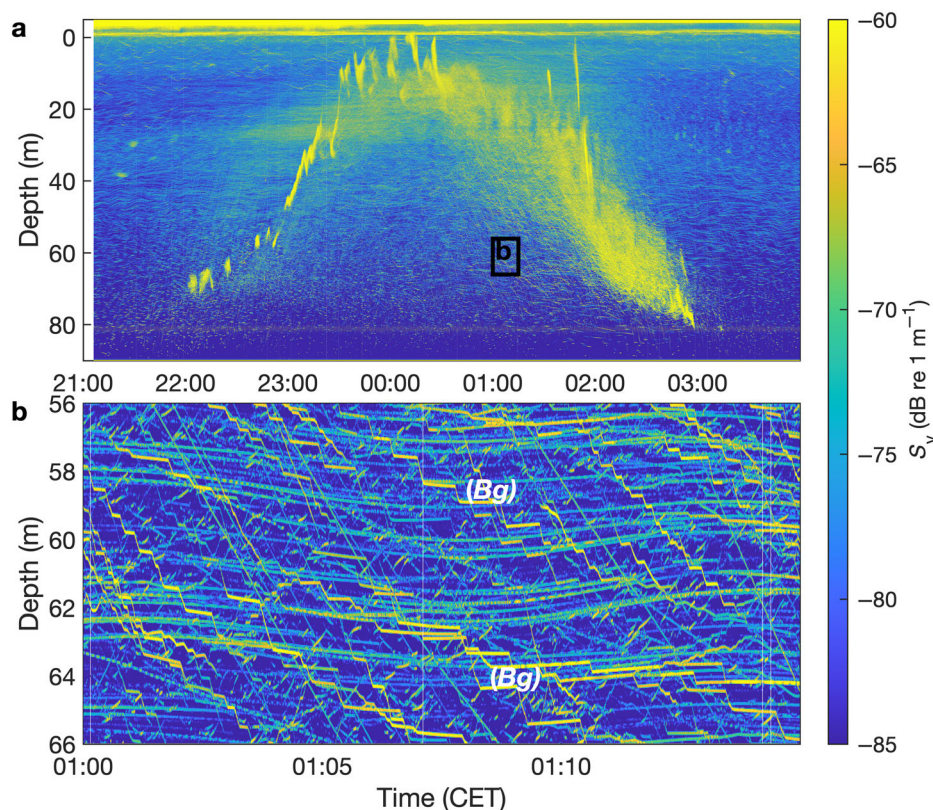
Fig. 5. Echograms (200 kHz) showing the upper 90 m of the water column on the night of 22 June 2011. (**a**) The main migration pattern of the schooling *Maurolicus muelleri* (pulsed echoes at 80 m is noise). The high-resolution excerpt (**b**) depicts individual stepwise migrating echo traces tentatively interpreted as *Benthosema glaciale* (*Bg*).

Vertical swimming was less noticeable near-bottom (tracking at 38 kHz) than in mid-waters. The tracking of all data by the bottom-mounted echosounder did not discern the ascent in the afternoon as displayed by individual echo traces (not shown).

Horizontal swimming was often associated with vertical relocation and limited during vertical pauses (Fig. 8). The swimming comprised turns and loops, with overall velocities reaching ~ 3 cm s^{-1} during active relocation, but with low velocities much of the time (Fig. 8). The tortuosity data reflected considerable deviation from straight swimming (Fig. 9). The fish were active in the horizontal plane during both day and night. However, horizontal speeds were slightly lower and pause durations longer at night (Figs. 7i,j, 9).

The individual horizontal swimming patterns recorded in near-bottom waters at 38 kHz appeared similar to those observed at 120 kHz, with stepwise swimming, turns, and loops (Supporting Information Fig. S4).

Discussion

B. glaciale was active during daytime in the twilight zone and displayed varying DVM patterns and individual timing of migrations relative to sunset and sunrise. The daytime swimming of *B. glaciale* observed here contrasts the notion of torpid mesopelagic fishes in the twilight zone (Barham 1971; Kaartvedt et al. 2009; Belcher et al. 2020), as did recent documentation for mesopelagic fishes in the Red Sea (Sobradillo et al. 2022). Yet, the stop-and-go behavior entailed longer pauses than the duration of periods for the relocations. The fishes in the Red Sea twilight zone appeared to move more continuously (Sobradillo et al. 2022).

The echo traces displayed individuals initiating their ascent one by one; some leaving near-bottom waters already ~ 4 h before sunset in foul and dark weather. Various taxa display size-related differences in migratory timing, with the smallest individuals starting ascent first (De Robertis et al. 2000; Benoit-Bird and Moline 2021). However, we found no increases in TS from early to late migrators, neither from the tracking at 265–275 m nor from TS derived from the tracks recorded between 255 and 305 m depth by the bottom-mounted echosounder. Instead, state-related factors such as gut fullness might explain the decision of individual mesopelagic organisms to migrate (Sutton and Hopkins 1996; Bos et al. 2021), and if applicable here may relate to foraging during the long summer days.
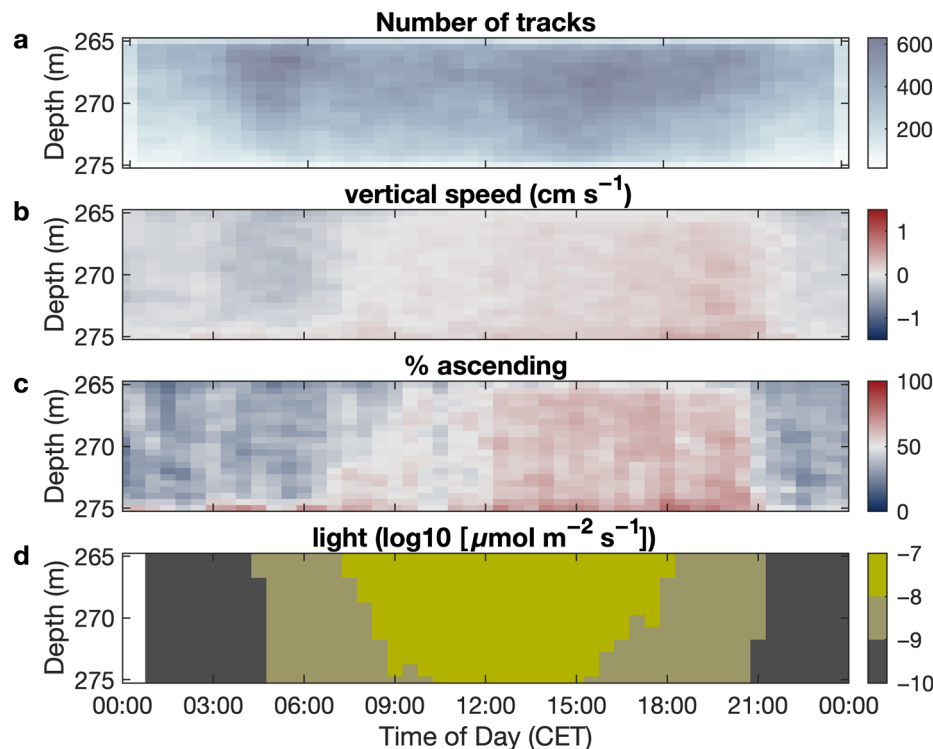
Fig. 6. Number of tracks (**a**), and vertical track properties (120 kHz) over time of day and depth (**b**, **c**) relative to estimated ambient light (**d**), averaged between 10 and 30 June 2011. Blue colors in (**b**) and (**c**) indicate prevailing downward swimming while red colors indicate a general ascending direction. Targets with target strength (TS; dB re 1 m^2) between −60 and −70 dB are included.

The initiation of ascent in the afternoon relates to light cues. Hypotheses for the proximate control of light on DVM include a preference for particular isolumes, the existence of an absolute intensity threshold, and responses to the relative rate of change (Cohen and Forward 2009). In addition, the concept of a light comfort zone relates to organisms actively avoiding both too-strong and too-low light (Røstad et al. 2016). The surface irradiance changes slowly at high latitudes in summer, in this case only ∼ 1.6 orders of magnitude during the extended period for the onset of migration. This would correspond to the estimated light extinction over a depth range of ∼ 40 m, which is only a small fraction of the vertical range of the population distribution. In the current study, both the daytime vertical distribution and the onset of migrations accord with the theory of a light comfort zone, which for the *B. glaciale* population encompasses 3–4 orders of magnitude (Røstad et al. 2016). For mesopelagic fishes that are dark-adapted visual predators, and themselves exposed to visual predators, this might reflect the evolutionary solution to the trade-off between visual foraging opportunities and predation mortality (Clark and Levy 1988; Røstad et al. 2016).

Wide vertical population distributions would not exclude the possibilities of individuals following their respective isolumes during DVM (Roe 1983; Frank and Widder 2002). However, the individual *B. glaciale* ascended considerably faster

than the slow ascent of isolumes (cf. Figure 2). We have used one value for light extinction, although solar elevation and sky conditions affect the angular distribution of light and thereby the extinction (Jerlov 1976). This introduces uncertainties, as does the extrapolation for the estimates of absolute light values at depth. Yet, the other mesopelagic fish in the fjord—*M. muelleri*—continuously adjusted its vertical distribution relative to incoming light within one order of magnitude, as also documented previously (Baliño and Aksnes 1993; Staby and Aksnes 2011). This coherence between depth variations suggests that the coarse patterns on isolume variations at depth are sufficiently reliable to justify the conclusion on individual migration rates relative to light.

Extrapolating echo traces ascending from near-bottom waters indicated that individual fish could reach upper layers shortly after sunset. Therefore, the short summer nights did not obstruct even the deepest living individuals. In the Southern Ocean, vertically migrating mesopelagic fishes ascended into the upper ∼ 200 m for foraging during short summer nights (Robison 2003). However, migrating past the 200 kHz echosounder located at 90 m would imply exposure to estimated nocturnal light levels > 10^{-6} μmol m^{-2} s^{-1} (roughly corresponding to the nocturnal irradiance at the 200 kHz echosounder; cf. Figure 1). This exceeds levels estimated for their daytime habitat in the twilight zone and their suggested
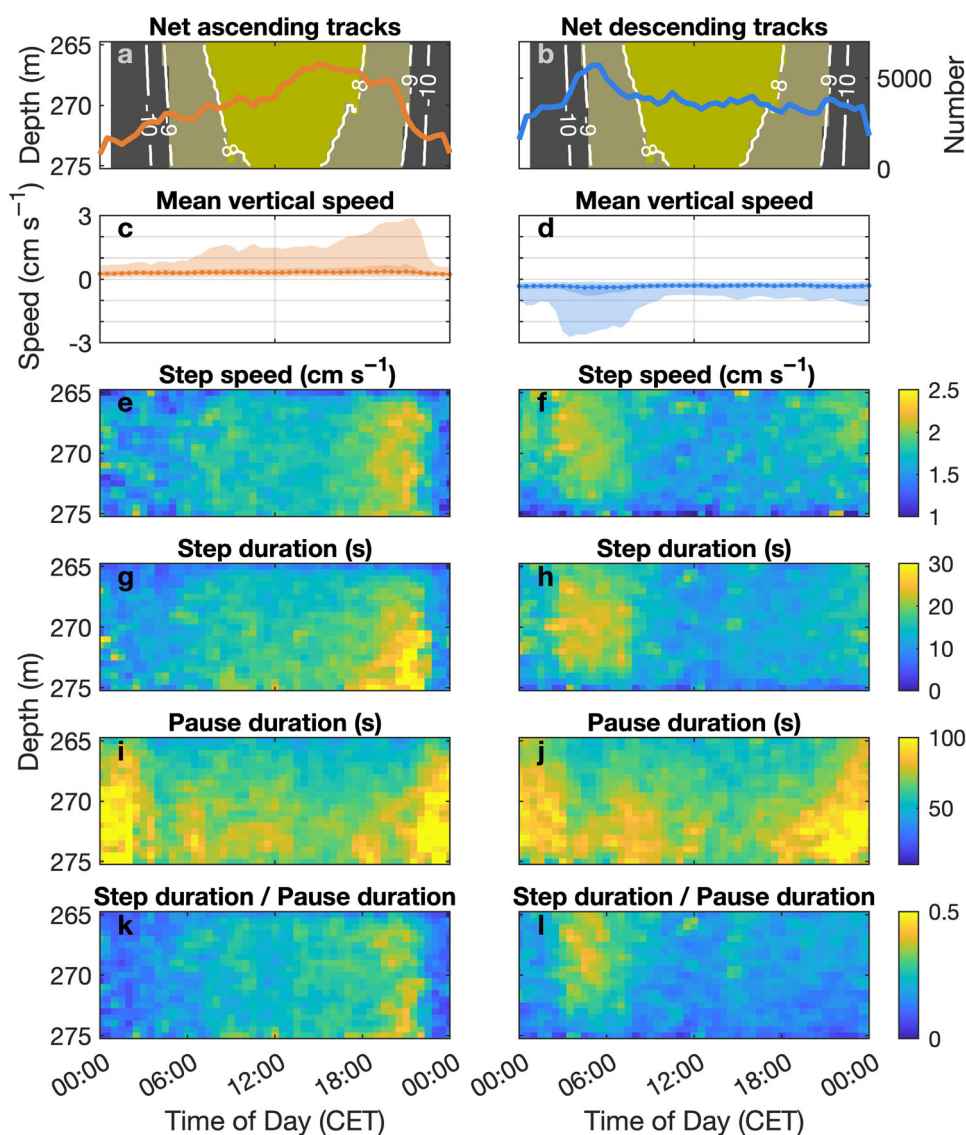
Fig. 7. Statistics for ascending (left column) and descending (right column) tracks over the diel cycle. (**a,b**) Number of tracks superimposed on estimated ambient light. (**c,d**) Median vertical speed with 25th and 75th (darker areas) and 5th and 95th (lighter areas) percentiles. (**e,f**) Speed during vertical steps, (**g,h**) duration of vertical steps, (**i,j**) duration of pauses between steps, (**k,l**) index of vertical activity depicting the relative time spent in steps vs. pauses.

light comfort zone (Figs. 1, 6, 7; Røstad et al. 2016). The 200 kHz echosounder unveiled stepwise ascending and descending targets, which we tentatively ascribe to *B. glaciale*. However, the interpretation of these data is challenging due to the diverse assemblage of targets. For example, *M. muelleri* also relocates vertically in a stepwise fashion (Christiansen et al. 2019), but it is mostly schooling in the upper layers in the light summer night (Prihartato et al. 2015; Fig. 5). In any case, the echosounder at 280 m recorded downward swimming of targets ascribed to *B. glaciale* early in the night, though at a slower speed than the downward pulse closer to sunrise (Fig. 7). This suggests that only a limited number of individuals might migrate to near-surface waters.

We show that fish in the twilight zone are relocating throughout long summer days, swimming both vertically and horizontally, involving turns and loops. The individual vertical daytime swimming concurs with previous reports on inverse vertical migrations of scattering layers ascribed to *B. glaciale* (Kaartvedt et al. 2009; Dypvik et al. 2012*b*). Lanternfishes boast light-sensitive eyes (Turner et al. 2009; de Busserolles et al. 2020) and likely *B. glaciale* can search visually at the estimated light intensities of their deep daytime habitat. Although vertically migrating *B. glaciale* typically forages in upper waters at night (Roe and Badcock 1984; Sameoto 1989; Pepin 2013), mesopelagic fishes also forage in their daytime habitat (Pearcy et al. 1979; Roe and Badcock 1984;
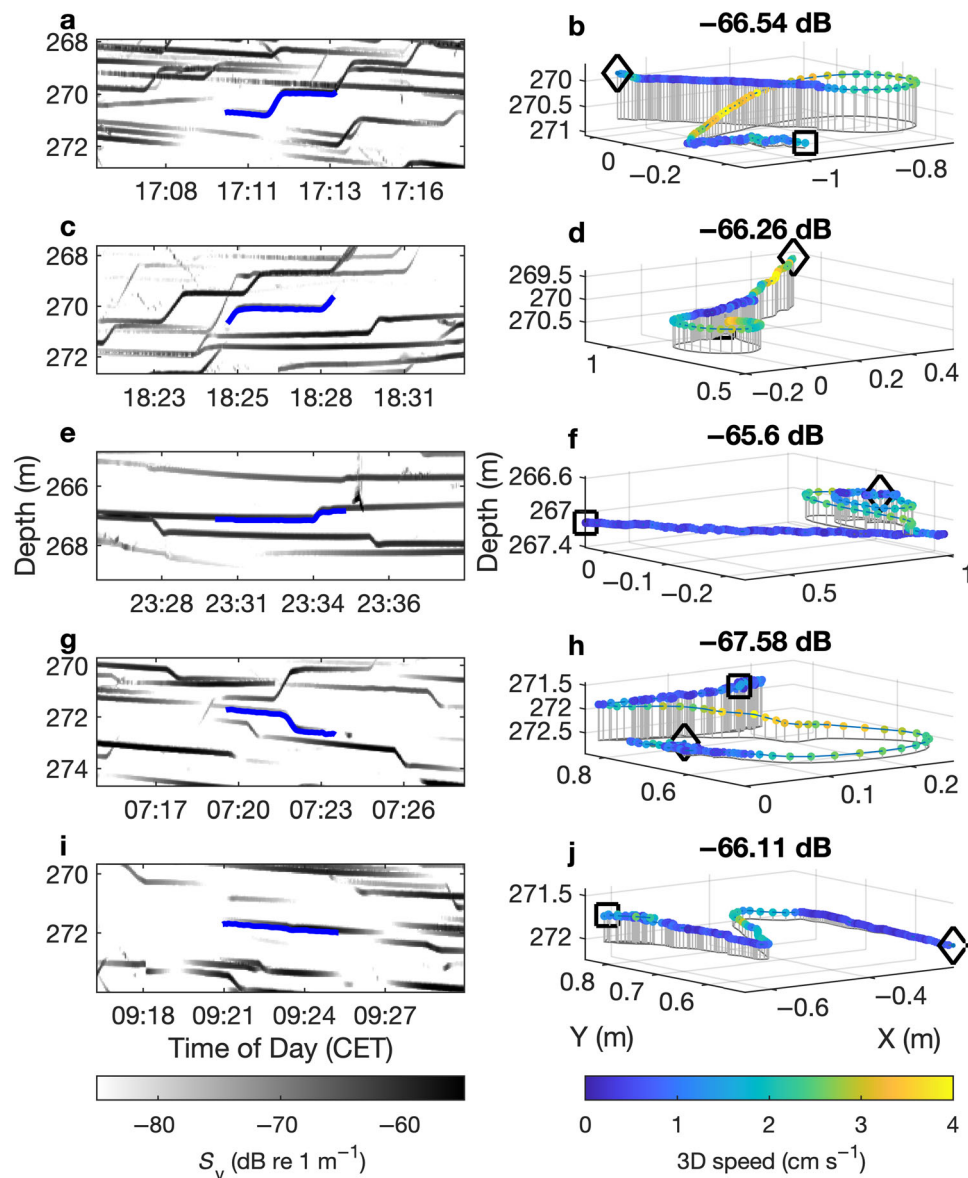
Fig. 8. Examples of echo traces (left) and the corresponding 3D tracks (right; the blue segment from trace) recorded by the 120 kHz echosounder. The start and end of each 3D track are marked by a square and diamond, respectively. The color of the dots represents the overall instantaneous speed of the track at that time point. The median target strength (dB) is depicted atop each track.

Sameoto 1988), as does *B. glaciale* in this fjord (Giske et al. 1990; Baliño and Aksnes 1993; Dypvik et al. 2012*b*). Light affects detection distance, and appears to limit food consumption more than the prey concentration does (Aksnes and Giske 1993), and Dypvik et al. (2012*b*) hypothesized that *B. glaciale* swims upward during the daytime to improve visual prey detection.

The nocturnal light in the upper waters of Masfjorden was higher than estimated for the daytime depths of *B. glaciale*. Correspondingly, and irrespective of latitude, surface light levels at full moon ($\sim 10^{-3}\ \mu\mathrm{mol\ m^{-2}\ s^{-1}}$) may be orders of magnitude higher than light levels at the upper part of the deep scattering layer (often termed DSL) in the daytime (Kaartvedt et al. 2019).

Therefore, division of light into the night-light and daylight is insufficient to characterize the habitats and distributional patterns of vertically migrating twilight organisms. The diel cycle may more involve changes in encounters with abundance and types of prey than changes in light. The abundance of zooplankton in near-surface waters may by far exceed that of potential deep-water prey. However, deep waters house larger potential prey such as krill, mysids, shrimps, and large copepods, particularly in daytime. A single krill may cover the daily energy requirement of a myctophid (Urmy and Horne 2016). With increasing size, prey items are more easily seen and, if active, can be detected hydrodynamically (O'Brien et al. 1990; Janssen et al. 1999).
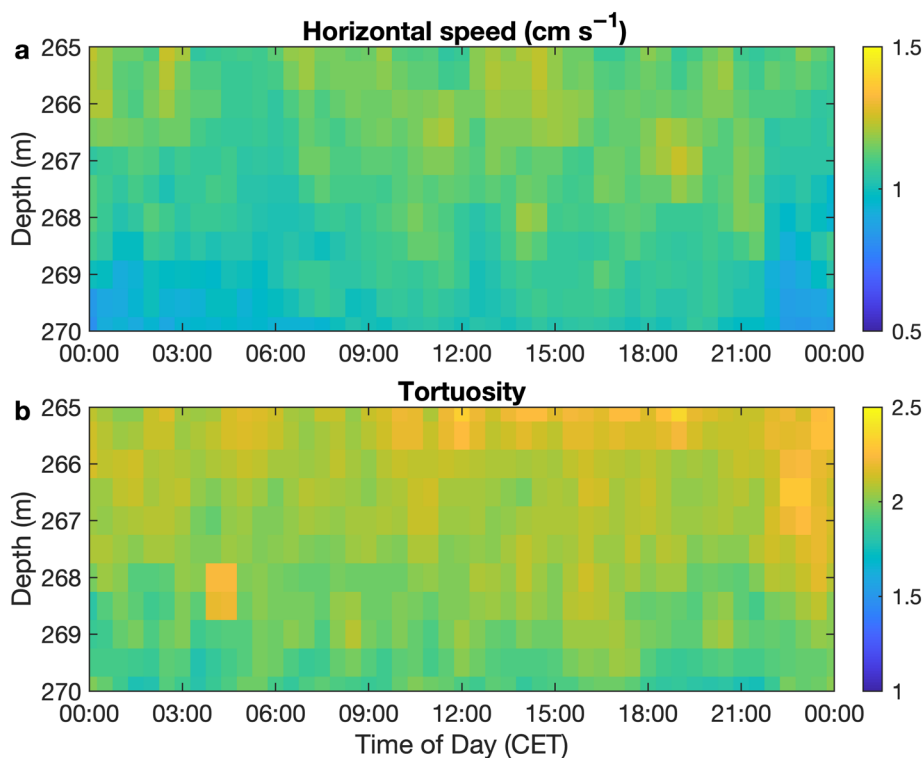
Fig. 9. Horizontal track properties over depth and time of day for tracks recorded at 120 kHz between 10 and 30 June 2011.

Activity levels and swimming patterns govern predator–prey interactions. The movements of *B. glaciale* as unveiled here comply with saltatory search, which works both for visual and nonvisual prey detection (O'Brien et al. 1990; Ryer and Olla 1999). The organisms move to new pastures and then scan for prey during the stationary phases. Changing both vertical distribution and directions may confuse predators (Christiansen et al. 2022). Success in exploiting resources in the twilight zone would affect possible constraints by photoperiod imposed at high latitudes, with bearing for questions like whether or not the constancy of light regime under climate change will prevent mesopelagic fishes from invading the Arctic (Kaartvedt 2008; Proud et al. 2017; Ljungström et al. 2021; Chawarski et al. 2022).

Modifying the concept of torpid daytime behavior of mesopelagic fishes also has implications in oceans beyond high latitudes. Swimming and foraging of mesopelagic fishes in the twilight zone will affect their conceived role in the biological carbon pump (Davison et al. 2013; Belcher et al. 2019; Pinti et al. 2022). Foraging during the daytime by vertically migrating fishes might entail an upward carbon transport modulating the expected net downward flux. In current models, fish-mediated vertical carbon export estimates are sensitive to the respiration (Davison et al. 2013; Saba et al. 2021), and hence to the accuracy of estimated activity levels (Torres and Somero 1988) at depth. Swimming moreover enhances the fishes' vulnerability to predators, like tactile, gelatinous

predators that abound in mid-water ecosystems (Choy et al. 2017; Robison et al. 2020). Pinti et al. (2022) highlighted the role of behavior and associated trophic interactions in mid-waters and the deep sea for estimates of global carbon fluxes, underlining the need for data from this part of the water column.

In conclusion, *B. glaciale* was active throughout the diel cycle, including the long summer days. The swimming behavior on both small scales within the twilight zone and larger DVM scales was plastic with individuals displaying various patterns. Although our understanding of the individual behavior of mesopelagic fishes is still in its infancy, the current approach of studying individual mesopelagic fishes in the twilight zone, recently also used in tropical waters (Sobradillo et al. 2022), provides a novel perspective for assessments of mesopelagic ecosystems worldwide. Overall, our study underscores the need for considering individual daytime behavior as well as flexible DVM patterns when evaluating the role of mesopelagic fishes in marine food webs, their active part of the carbon pump, and for assessing responses to climate change.

Data availability statement

References

Aksnes, D. L. 2021. Light measurements in Masfjorden 2010–2011, western Norway. doi:10.1594/PANGAEA.932328

Aksnes, D. L., and J. Giske. 1993. A theoretical model of aquatic visual feeding. Ecol. Model. **67**: 233–250. doi:10.1016/0304-3800(93)90007-F

Aksnes, D. L., J. Aure, P.-O. Johansen, G. H. Johnsen, and A. G. Vea Salvanes. 2019. Multi-decadal warming of Atlantic water and associated decline of dissolved oxygen in a deep fjord. Est. Coast. Shelf Sci. **228**: 106392. doi:10.1016/j.ecss.2019.106392

Baliño, B. M., and D. L. Aksnes. 1993. Winter distribution and migration of the sound scattering layers, zooplankton and micronekton in Masfjorden, western Norway. Mar. Ecol. Prog. Ser. **95**: 35–50.

Balk, H. 2019. Sonar4 and Sonar5-Pro post processing systems. Operator manual version 606.16. CageEye AS.

Balk, H., and T. Lindem. 2002. A new method for single target detection, p. 1–9. *In* Proceedings of the ICES 6th Symposium on Acoustics in Fisheries and Aquatic Ecology. Montpellier, France.

Barham, E. G. 1966. Deep scattering layer migration and composition: observations from a diving saucer. Science **151**: 1399–1403.

Barham, E. G. 1971. Deep-sea fishes. Lethargy and vertical orientation, p. 100–118. *In* Proceedings of International Symposium on Biological Sound Scattering in the Ocean. United States Government Publishing Office.

Belcher, A., R. Saunders, and G. Tarling. 2019. Respiration rates and active carbon flux of mesopelagic fishes (Family Myctophidae) in the Scotia Sea, Southern Ocean. Mar. Ecol. Prog. Ser. **610**: 149–162. doi:10.3354/meps12861

Belcher, A., K. Cook, D. Bondyale-Juez, G. Stowasser, S. Fielding, R. A. Saunders, D. J. Mayor, and G. A. Tarling. 2020. Respiration of mesopelagic fish: a comparison of respiratory electron transport system (ETS) measurements and allometrically calculated rates in the Southern Ocean and Benguela Current. ICES J. Mar. Sci. **77**: 1672–1684. doi:10.1093/icesjms/fsaa031

Benoit-Bird, K. J., and M. A. Moline. 2021. Vertical migration timing illuminates the importance of visual and nonvisual predation pressure in the mesopelagic zone. Limnol. Oceanogr. **66**: 3010–3019. doi:10.1002/lno.11855

Bianchi, D., and K. A. S. Mislan. 2016. Global patterns of diel vertical migration times and velocities from acoustic data: Global patterns of diel vertical migration. Limnol. Oceanogr. **61**: 353–364. doi:10.1002/lno.10219

Bos, R. P., T. T. Sutton, and T. M. Frank. 2021. State of Satiation Partially Regulates the Dynamics of Vertical Migration. Front. Mar. Sci. **8**: 607228. doi:10.3389/fmars.2021.607228

Brede, R., F. H. Kristensen, H. Solli, and E. Ona. 1990. Target tracking with a split-beam echo sounder. Rapp. PV. Reùn Cons. Int. Explor. Mer. **189**: 254–263.

de Busserolles, F., and others. 2017. Pushing the limits of photoreception in twilight conditions: The rod-like cone retina of the deep-sea pearlsides. Sci. Adv. **3**: eaao4709. doi:10.1126/sciadv.aao4709

de Busserolles, F., L. Fogg, F. Cortesi, and J. Marshall. 2020. The exceptional diversity of visual adaptations in deep-sea teleost fishes. Semin. Cell Dev. Biol. **106**: 20–30. doi:10.1016/j.semcdb.2020.05.027

Chawarski, J., T. A. Klevjer, D. Coté, and M. Geoffroy. 2022. Evidence of temperature control on mesopelagic fish and zooplankton communities at high latitudes. Front. Mar. Sci. **9**: 917985. doi:10.3389/fmars.2022.917985

Choy, C. A., S. H. D. Haddock, and B. H. Robison. 2017. Deep pelagic food web structure as revealed by *in situ* feeding observations. Proc. R. Soc. B Biol. Sci. **284**: 20172116. doi:10.1098/rspb.2017.2116

Christiansen, S., J. Titelman, and S. Kaartvedt. 2019. Nighttime swimming behavior of a mesopelagic fish. Front. Mar. Sci. **6**: 1–12. doi:10.3389/fmars.2019.00787

Christiansen, S., T. A. Klevjer, A. Røstad, D. L. Aksnes, and S. Kaartvedt. 2021. Flexible behaviour in a mesopelagic fish (*Maurolicus muelleri*). ICES J. Mar. Sci. **78**: 1623–1635. doi:10.1093/icesjms/fsab075

Christiansen, S., Ø. Langangen, and S. Kaartvedt. 2022. Three-dimensional swimming behavior and activity of a mesopelagic fish. Limnol. Oceanogr. **67**: 2677–2690. doi:10.1002/lno.12230

Clark, C. W., and D. A. Levy. 1988. Diel vertical migrations by juvenile sockeye salmon and the antipredation window. Am. Nat. **131**: 271–290.

Cohen, J. H., and R. B. Forward. 2009. Zooplankton diel vertical migration—A review of proximate control, p. 77–109. *In* Oceanography and marine biology: An annual review. CRC Press.

Davison, P. C., D. M. Checkley, J. A. Koslow, and J. Barlow. 2013. Carbon export mediated by mesopelagic fishes in the northeast Pacific Ocean. Prog. Oceanogr. **116**: 14–30. doi:10.1016/j.pocean.2013.05.013

De Robertis, A., J. S. Jaffe, and M. D. Ohman. 2000. Size-dependent visual predation risk and the timing of vertical migration in zooplankton. Limnol. Oceanogr. **45**: 1838–1844. doi:10.4319/lo.2000.45.8.1838

Du Clos, K. T., B. J. Gemmell, S. P. Collin, J. H. Costello, J. O. Dabiri, and K. R. Sutherland. 2022. Distributed propulsion enables fast and efficient swimming modes in physonect siphonophores. PNAS **119**: e2202494119. doi:10.1073/pnas.2202494119

Dypvik, E., A. Røstad, and S. Kaartvedt. 2012*a*. Seasonal variations in vertical migration of glacier lanternfish, *Benthosema glaciale*. Mar. Biol. **159**: 1673–1683. doi:10.1007/s00227-012-1953-2

Dypvik, E., T. A. Klevjer, and S. Kaartvedt. 2012*b*. Inverse vertical migration and feeding in glacier lanternfish (*Benthosema glaciale*). Mar. Biol. **159**: 443–453. doi:10.1007/s00227-011-1822-4

Foote, K., H. Knudsen, G. Vestnes, D. MacLennan, and E. Simmonds. 1987. Calibration of acoustic instruments for fish density estimation: a practical guide. ICES Coop. Res. Rep. **144**: 1–69.

Frank, T. M., and E. A. Widder. 2002. Effects of a decrease in downwelling irradiance on the daytime vertical distribution patterns of zooplankton and micronekton. Mar. Biol. **140**: 1181–1193. doi:10.1007/s00227-002-0788-7

Fujino, T., K. Sadayasu, K. Abe, H. Kidokoro, Y. Tian, H. Yasuma, and K. Miyashita. 2009. Swimbladder morphology and target strength of a mesopelagic fish, *Maurolicus japonicus*. J. Marine Acoust. Soc. Jpn. **36**: 241–249. doi:10.3135/jmasj.36.241

Gerritsen, J., and J. R. Strickler. 1977. Encounter probabilities and community structure in zooplankton: A mathematical model. J. Fish. Res. Board Can. **34**: 73–82. doi:10.1139/f77-008

Giske, J., and others. 1990. Vertical distribution and trophic interactions of zooplankton and fish in Masfjorden, Norway. Sarsia **75**: 65–81. doi:10.1080/00364827.1990.10413442

Godø, O. R., R. Patel, and G. Pedersen. 2009. Diel migration and swimbladder resonance of small fish: some implications for analyses of multifrequency echo data. ICES J. Mar. Sci. **66**: 1143–1148. doi:10.1093/icesjms/fsp098

Greenlaw, C. F. 1977. Backscattering spectra of preserved zooplankton. J. Acoust. Soc. Am. **62**: 44–52.

Halliday, R. G. 1970. Growth and Vertical Distribution of the Glacier Lanternfish, *Benthosema glaciale*, in the Northwestern Atlantic. J. Fish. Res. Board Can. **27**: 105–116. doi:10.1139/f70-011

Hays, G. C. 2003. A review of the adaptive significance and ecosystem consequences of zooplankton diel vertical migrations. Hydrobiologia **503**: 163–170. doi:10.1023/B:HYDR.0000008476.23617.b0

Hetherington, E. D., A. Damian-Serrano, S. H. D. Haddock, C. W. Dunn, and C. A. Choy. 2022. Integrating siphonophores into marine food-web ecology. Limnol. Oceanogr. Lett. **7**: 81–95.

Hosia, A., and U. Båmstedt. 2008. Seasonal abundance and vertical distribution of siphonophores in western Norwegian fjords. J. Plankton Res. **30**: 951–962. doi:10.1093/plankt/fbn045

Hudson, J. M., D. K. Steinberg, T. T. Sutton, J. E. Graves, and R. J. Latour. 2014. Myctophid feeding ecology and carbon transport along the northern Mid-Atlantic Ridge. Deep Sea Res. I Ocenogr. Res. Pap. **93**: 104–116. doi:10.1016/j.dsr.2014.07.002

Janssen, J., V. Sideleva, and H. Biga. 1999. Use of the lateral line for feeding in two Lake Baikal sculpins. J. Fish Biol. **54**: 404–416. doi:10.1111/j.1095-8649.1999.tb00839.x

Jerlov, N. G. 1976. Marine optics. Elsevier.

Kaartvedt, S. 2008. Photoperiod may constrain the effect of global warming in arctic marine systems. J. Plankton Res. **30**: 1203–1206. doi:10.1093/plankt/fbn075

Kaartvedt, S., T. Knutsen, and J. Holst. 1998. Schooling of the vertically migrating mesopelagic fish *Maurolicus muelleri* in light summer nights. Mar. Ecol. Prog. Ser. **170**: 287–290. doi:10.3354/meps170287

Kaartvedt, S., T. Torgersen, T. A. Klevjer, A. Røstad, and J. Devine. 2008. Behavior of individual mesopelagic fish in acoustic scattering layers of Norwegian fjords. Mar. Ecol. Prog. Ser. **360**: 201–209. doi:10.3354/meps07364

Kaartvedt, S., A. Røstad, T. A. Klevjer, and A. Staby. 2009. Use of bottom-mounted echo sounders in exploring behavior of mesopelagic fishes. Mar. Ecol. Prog. Ser. **395**: 109–118. doi:10.3354/meps08174

Kaartvedt, S., T. J. Langbehn, and D. L. Aksnes. 2019. Enlightening the oceans' twilight zone. ICES J. Mar. Sci. **76**: 803–812. doi:10.1093/icesjms/fsz010

Kaartvedt, S., B. Sobradillo Benguria, T. A. Klevjer, and A. Røstad. 2021. Cabled acoustic observatory. doi:10.21335/NMDC-1243831716

Kays, R., M. C. Crofoot, W. Jetz, and M. Wikelski. 2015. Terrestrial animal tracking as an eye on life and planet. Science **348**: aaa2478-1–aaa2478-9. doi:10.1126/science.aaa2478

Klevjer, T. A., X. Irigoien, A. Røstad, E. Fraile-Nuez, V. M. Benítez-Barrios, and S. Kaartvedt. 2016. Large scale patterns in vertical distribution and behaviour of mesopelagic scattering layers. Sci. Rep. **6**: 1–11. doi:10.1038/srep19873

Langbehn, T. J., D. L. Aksnes, S. Kaartvedt, Ø. Fiksen, G. Ljungström, C. Jørgensen, and A. Bates. 2022. Poleward distribution of mesopelagic fishes is constrained by seasonality in light. Glob. Ecol. Biogeogr. **31**: 546–561. doi:10.1111/geb.13446

Ljungström, G., T. J. Langbehn, and C. Jørgensen. 2021. Light and energetics at seasonal extremes limit poleward range shifts. Nat. Clim. Change **11**: 530–536. doi:10.1038/s41558-021-01045-2

Love, R. H., R. A. Fisher, M. A. Wilson, and R. W. Nero. 2004. Unusual swimbladder behavior of fish in the Cariaco Trench. Deep Sea Res. I Ocenogr. Res. Pap. **51**: 1–16. doi:10.1016/j.dsr.2003.09.004

Norheim, E., T. A. Klevjer, and D. L. Aksnes. 2016. Evidence for light-controlled migration amplitude of a sound scattering layer in the Norwegian Sea. Mar. Ecol. Prog. Ser. **551**: 45–52. doi:10.3354/meps11731

O'Brien, W. J., H. I. Browman, and B. I. Evans. 1990. Search strategies of foraging animals. Am. Sci. **78**: 152–160.

Olivar, M. P., A. Bernal, B. Molí, M. Peña, R. Balbín, A. Castellón, J. Miquel, and E. Massutí. 2012. Vertical distribution, diversity and assemblages of mesopelagic fishes in the western Mediterranean. Deep Sea Res. I Oceanogr. Res. Pap. **62**: 53–69. doi:10.1016/j.dsr.2011.12.014

Olivar, M. P., P. A. Hulley, A. Castellon, M. Emelianov, C. Lopez, V. M. Tuset, T. Contreras, and B. Moli. 2017. Mesopelagic fishes across the tropical and equatorial Atlantic: Biogeographical and verticalpatterns. Prog. Oceanogr. **151**: 116–137. doi:10.1016/j.pocean.2016.12.001

Pearcy, W. G., H. V. Lorz, and W. Peterson. 1979. Comparison of the feeding habits of migratory and non-migratory *Stenobrachius leucopsarus* (Myctophidae). Mar. Biol. **51**: 1–8. doi:10.1007/BF00389025

Pearre, S. 2003. Eat and run? The hunger/satiation hypothesis in vertical migration: history, evidence and consequences. Biol. Rev. **78**: 1–79. doi:10.1017/S146479310200595X

Peña, M., J. Cabrera-Gámez, and A. C. Domínguez-Brito. 2020. Multi-frequency and light-avoiding characteristics of deep acoustic layers in the North Atlantic. Mar. Environ. Res. **154**: 104842. doi:10.1016/j.marenvres.2019.104842

Pepin, P. 2013. Distribution and feeding of *Benthosema glaciale* in the western Labrador Sea: Fish–zooplankton interaction and the consequence to calanoid copepod populations. Deep Sea Res. I Oceanogr. Res. Pap. **75**: 119–134. doi:10.1016/j.dsr.2013.01.012

Pinti, J., A. W. Visser, C. Serra-Pompei, K. H. Andersen, M. D. Ohman, and T. Kiørboe. 2022. Fear and loathing in the pelagic: How the seascape of fear impacts the biological carbon pump. Limnol. Oceanogr. **67**: 1238–1256. doi:10.1002/lno.12073

Prihartato, P., D. L. Aksnes, and S. Kaartvedt. 2015. Seasonal patterns in the nocturnal distribution and behavior of the mesopelagic fish *Maurolicus muelleri* at high latitudes. Mar. Ecol. Prog. Ser. **521**: 189–200. doi:10.3354/meps11139

Proud, R., M. J. Cox, and A. S. Brierley. 2017. Biogeography of the global ocean's Mesopelagic zone. Curr. Biol. **27**: 113–119. doi:10.1016/j.cub.2016.11.003

Proud, R., N. O. Handegard, R. J. Kloser, M. J. Cox, and A. S. Brierley. 2019. From siphonophores to deep scattering layers: uncertainty ranges for the estimation of global mesopelagic fish biomass. ICES J. Mar. Sci. **76**: 718–733. doi:10.1093/icesjms/fsy037

Rasmussen, O. I., and J. Giske. 1994. Life-history parameters and vertical distribution of *Maurolicus muelleri* in Masfjorden in summer. Mar. Biol. **120**: 649–664. doi:10.1007/BF00350086

Robison, B. H. 2003. What drives the diel vertical migrations of Antarctic midwater fish? J. Mar. Biol. Assoc. U.K. **83**: 639–642. doi:10.1017/S0025315403007586h

Robison, B. H., R. E. Sherlock, K. R. Reisenbichler, and P. R. McGill. 2020. Running the Gauntlet: Assessing the threats to vertical migrators. Front. Mar. Sci. **7**: 1–10. doi:10.3389/fmars.2020.00064

Roe, H. S. J. 1983. Vertical distributions of euphausiids and fish in relation to light intensity in the Northeastern Atlantic. Mar. Biol. **77**: 287–298. doi:10.1007/BF00395818

Roe, H. S. J., and J. Badcock. 1984. The diel migrations and distributions within a mesopelagic community in the North East Atlantic. 5. Vertical migrations and feeding of fish. Prog. Oceanogr. **13**: 389–424. doi:10.1016/0079-6611(84)90014-4

Røstad, A., S. Kaartvedt, and D. L. Aksnes. 2016. Light comfort zones of mesopelagic acoustic scattering layers in two contrasting optical environments. Deep Sea Res. I Oceanogr. Res. Pap. **113**: 1–6. doi:10.1016/j.dsr.2016.02.020

Ryer, C., and B. Olla. 1999. Light-induced changes in the prey consumption and behavior of two juvenile planktivorous fish. Mar. Ecol. Prog. Ser. **181**: 41–51. doi:10.3354/meps181041

Saba, G. K., and others. 2021. Toward a better understanding of fish-based contribution to ocean carbon flux. Limnol. Oceanogr. **66**: 1639–1664. doi:10.1002/lno.11709

Sameoto, D. 1988. Feeding of lantern fish *Benthosema glaciale* off the Nova Scotia Shelf. Mar. Ecol. Prog. Ser. **44**: 113–129. doi:10.3354/meps044113

Sameoto, D. 1989. Feeding ecology of the lantern fish *Benthosema glaciale* in a subarctic region. Polar Biol. **9**: 169–178. doi:10.1007/BF00297172

Sarmiento-Lezcano, A. N., M. P. Olivar, M. Peña, J. M. Landeira, L. Armengol, I. Medina-Suárez, A. Castellón, and S. Hernández-León. 2022. Carbon remineralization by small mesopelagic and bathypelagic Stomiiforms in the Northeast Atlantic Ocean. Prog. Oceanogr. **203**: 102787. doi:10.1016/j.pocean.2022.102787

Scoulding, B., D. Chu, E. Ona, and P. G. Fernandes. 2015. Target strengths of two abundant mesopelagic fish species. J. Acoust. Soc. Am. **137**: 989–1000.

Sobradillo, B., S. Christiansen, A. Røstad, and S. Kaartvedt. 2022. Individual daytime swimming of mesopelagic fishes in the world's warmest twilight zone. Deep Sea Res. I Oceanogr. Res. Pap. **190**: 103897. doi:10.1016/j.dsr.2022.103897

Staby, A., and D. L. Aksnes. 2011. Follow the light—diurnal and seasonal variations in vertical distribution of the mesopelagic fish *Maurolicus muelleri*. Mar. Ecol. Prog. Ser. **422**: 265–273. doi:10.3354/meps08938

Staby, A., A. Røstad, and S. Kaartvedt. 2011. Long-term acoustical observations of the mesopelagic fish *Maurolicus muelleri* reveal novel and varied vertical migration patterns. Mar. Ecol. Prog. Ser. **441**: 241–255. doi:10.3354/meps09363

Sutton, T. T., and T. L. Hopkins. 1996. Trophic ecology of the stomiid (Pisces: Stomiidae) fish assemblage of the eastern Gulf of Mexico: Strategies, selectivity and impact of a top mesopelagic predator group. Mar. Biol. **127**: 179–192. doi:10.1007/BF00942102

Torres, J. J., B. W. Belman, and J. J. Childress. 1979. Oxygen consumption rates of midwater fishes as a function of depth of occurrence. Deep Sea Res. A Oceanogr. Res. Pap. **26A**: 185–197. doi:10.1016/0198-0149(79)90075-X

Torres, J. J., and G. N. Somero. 1988. Vertical distribution and metabolism in Antarctic mesopelagic fishes. Comp. Biochem. Physiol. B Comp. Biochem. **90**: 521–528. doi:10.1016/0305-0491(88)90291-X

Turner, J. R., E. M. White, M. A. Collins, J. C. Partridge, and R. H. Douglas. 2009. Vision in lanternfish (Myctophidae): Adaptations for viewing bioluminescence in the deep-sea. Deep Sea Res. I Oceanogr. Res. Pap. **56**: 1003–1017. doi:10.1016/j.dsr.2009.01.007

Underwood, M. J., A. C. Utne Palm, J. T. Øvredal, and Å. Bjordal. 2021. The response of mesopelagic organisms to artificial lights. Aquacult. Fish. **6**: 519–529. doi:10.1016/j. aaf.2020.05.002

Urmy, S. S., and J. K. Horne. 2016. Multi-scale responses of scattering layers to environmental variability in Monterey Bay, California. Deep Sea Res. I Oceanogr. Res. Pap. **113**: 22–32. doi:10.1016/j.dsr.2016.04.004

Acknowledgments

Conflict of Interest

None declared.